ChemMedChem

Chemistry Europe
European Chemical Societies Publishing

Accepted Article

Title: Synthesis and structure-activity relationship of 3-arylisoquinolone analogues as novel highly specific hCES2A inhibitors

Authors: Bo Li, Yitian Zhao, Yuan Xiong, Sanfeng Dong, Xiaoqing Guan, Yunqing Song, Yanqing Yang, Kun Zou, Zhao Li, Yong Zhang, Shengquan Fang, Weiliang Zhu, Kaixian Chen, Qi Jia, and Guangbo Ge

To be cited as: *ChemMedChem* 10.1002/cmdc.202000581

Link to VoR: https://doi.org/10.1002/cmdc.202000581

WILEY-VCH

WILEY-VCH

FULL PAPER

Synthesis and structure-activity relationship of 3-arylisoquinolone analogues as novel highly specific hCES2A inhibitors

Yitian Zhao [a,b,#], Yuan Xiong [a,#], Sanfeng Dong [a,b,#], Xiaoqing Guan [a,#], Yunqing Song [a], Yanqing Yang [b], Kun Zou [b], Zhao Li [b], Yong Zhang [b], Shengquan Fang [a], Bo Li [b,*], Weiliang Zhu [a,b], Kaixian Chen [a,b], Qi Jia [a,*] , Guangbo Ge [a,*]

[a] Y. Zhao, Y. Xiong, S. Dong, X. Guan, Y. Song, S. Fang, Prof. W. Zhu, Prof. K. Chen, A/Prof. Q. Jia, Prof. G. Ge
Shanghai University of Traditional Chinese Medicine
1200 Cailun Road, Shanghai 201203, China
E-mail: geguangbo@dicp.ac.cn (Guangbo Ge)
q_jia@126.com (Qi JIA)

[b] Y. Zhao, S. Dong, Y. Yang, K. Zou, Z. Li, Y. Zhang, A/Prof. B. Li, Prof. W. Zhu, Prof. K. Chen,
CAS Key Laboratory of Receptor Research; Drug Discovery and Design Center
Shanghai Institute of Materia Medica, Chinese Academy of Sciences
555 Zuchongzhi Road, Shanghai 201203, China
E-mail: boli@simm.ac.cn (Bo Li)
# These authors contributed equally.

Abstract: Mammalian carboxylesterases (CES) are key enzymes participating in the hydrolytic metabolism of various endogenous and exogenous substrates. Human carboxylesterases 2A (hCES2A), mainly distributed in the small intestine and colon, plays a significant role in the hydrolysis of many drugs. In this study, 3-arylisoquinolones **3h** and **4a** were found with potent inhibitory effect on hCES2A (IC_{50} = 0.68 μM, K_i =0.36 μM) and excellent specificity (more than 147.05 fold over hCES1A). Moreover, **4a** exhibited 3-fold improvement inhibition on intracellular hCES2A in living HepG2 cells compared with **3h**, with the IC_{50} value of 0.41 μM. The inhibition kinetics results and molecular docking simulations demonstrated that both **3h** and **4a** could bind to multiple sites of hCES2A**,** functioning as mixed inhibitors. The SAR (structure-activity relationship) analysis revealed that the lactam moiety on B ring is crucial to the specificity towards hCES2A, while the benzyloxy group is the optimal group for hCES2A inhibition potency, and the introduction of bromine atom may enhance the permeability to increase the intracellular hCES2A inhibitory activity.

Introduction

Mammalian carboxylesterases (CES, EC. 3.1.1.1) are ubiquitous hydrolases located in the lumen of endoplasmic reticulum of many tissues. As one of the most important classes of serine hydrolases, CES play significant roles in catalysing the hydrolysis of various endogenous and exogenous substrates bearing ester, amide, thioester or carbamate bond(s).[1] In the human body, hCES1A and hCES2A are the most important hCES isoenzymes and their biological functions and substrate specificity have been extensively investigated.[2]

As the dominant esterase in the intestinal system, hCES2A participates in the hydrolysis of many therapeutic drugs, such as irinotecan, flutamide, dabigatran etexilate and capecitabine.[3] Over the past few decades, increasing evidence has indicated that the inhibition of intestinal hCES2A may improve the oral bioavailability or to alleviate the intestinal toxicity of some hCES2A-substrate drugs.[4] For example, loperamide, an anti-diarrheal medicine clinically used to ameliorate the intestinal toxicity caused by irinotecan, has been demonstrated to be a specific inhibitor of hCES2A.[5] Currently, many potent hCES2A inhibitors have been reported, such as bisbenzene sulphonamide[6] and benzil, but most of them have poor selectivity or cell-permeability.[5b, 7] Considering that hCES2A is an intracellular enzyme located in the lumen of endoplasmic reticulum, the agents with poor cell-permeability cannot displayed strong effects in living systems. Therefore, the novel specific hCES2A inhibitors with cell-permeability are highly desirable.

Compounds with the basic skeleton of isoquinolone possess broad biological activities.[8] Among them, 3-arylisoquinolones are commonly reported as the anticancer ingredients, while their inhibition against hCES have not been researched. The present study showed compound **3a**[9] (Fig. 1) could selectively inhibited hCES2A with moderate activity. However, the substitution of the hydrogen at the 2-position resulted in the loss of selectivity (**3a'** (Fig. 1)).[10] According to this result 13 analogues of **3a** were synthesized and **3h** was obtained with the obviously improved hCES2A inhibitory effects and excellent selectivity (Fig. 2)

Introduction of halogen could increase the lipophilicity of molecule to improve the permeability.[11] Therefore, we further synthesized a series of halogenated products of **3h** and the brominated product **4a** exhibited 3-fold improvement inhibition in the intracellular hCES2A inhibition assays, suggesting the introduction of the bromine atom led to an increase of lipophilicity which may enhance the cell-permeability. Meanwhile, the study of structure-activity relationships (SAR) and molecular docking simulations revealed the key functional groups that would be beneficial for hCES2A inhibition and specificity. All these researches showed that 3-arylisoquinolones could provide ideal leading compounds for the development of specific hCES2A inhibitors with high potency.

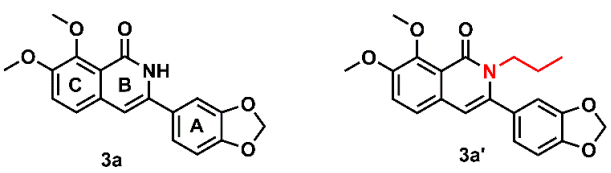

Figure 1. The structures of compounds **3a**, **3a'**.

Results and Discussion

Chemistry

3-arylisoquinolones **3b**, **3e**-**3n** (Fig. 2) were obtained based on our previous synthetic routes (Scheme 1). The intermediate **1a** was synthesized according to the method of Eliel et al. (Scheme 2).[12] To obtain **1b**, the synthetic route was optimized (Scheme 2). Commercially available benzoic acid derivative **14** was converted to the bromobenzoic acid **15** with 1,3-dibromo-5,5-dimethylhydantoin, followed by amidation to produce amide **16**. After that, compound **16** was subjected to lithiation at -78 °C, and then the mixture was treated with methyl iodide to afford the intermediate **1b**.[13]

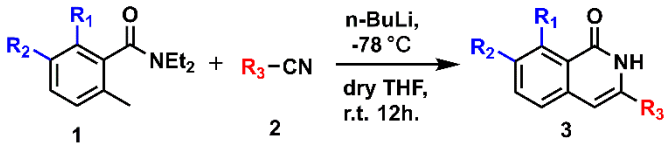

Scheme 1. Synthesis of **3a-3b**, **3e-3n**. Reagents and conditions: a) n-BuLi (-78 °C), dry THF, r.t. 12h.

After preliminary inhibitory activity screening of a series of 3-arylisoquinolone analogues against hCES, **3h** exhibited the strongest inhibitory activity with good selectivity (hCES1A IC_{50} >100 μM; hCES2A IC_{50} = 0.68 ± 0.07 μM). However, the poor yield (9% yield even worse) of **3h** impeded the next halogenation. For this reason, another efficient route was developed to prepare compound **3h** (Scheme 3). Firstly, the chlorine atom at 1-position of **5b** was selectively substituted with methoxy to give **6b**. The intermediate **7c** was synthesized via Suzuki coupling reaction between compound **6b** and (4-(benzyloxy)-3-methoxyphenyl) boronic acid. **7c** underwent demethylation by TMSCl and NaI to give **3h**. Finally, **4a** and **4b** were accomplished by treating **3h** with NBS and NCS respectively. The intermediate **7c** was chosen to be fluorinated or iodinated to give the corresponding products **8a** and **8b** respectively, which experienced demethylation to give **4c** and **4d**.

3c and **3d** were synthesized according to the routes mentioned above. The key intermediates **5b** and **5c** were synthesized through the synthetic routes outlined in scheme 4. Intramolecular Friedel-Crafts acylation of 3,4,5-trimethoxyphenylpropionic acid **20** at 50 °C with phosphorus pentoxide in methane sulfonic acid produced indanone **21a**. **21a** was treated with butyl nitrite under acidic conditions to get ketoxime **22**.[14] Then, **22** was transformed with sodium hydroxide and TsCl to generate **23** which was cyclized and chlorinated with PCl_5 and $POCl_3$ to provide the intermediate **5c**.[15]

5b couldn't be prepared *via* the same route as **5c** because the expected starting material **21b** was hard to obtain. Therefore, the synthesis of **5b** started from the intermediate **10** (scheme 4). For safety and convenience, methyl chloroformate was replaced with propyl chloroformate to give the compound **11b**. Subsequently, cyanation of **11b** with trimethylsilyl cyanide and tetrabutylammonium fluoride afforded **17**. Addition of methoxy anion to the nitrile moiety of **17** and cyclization gave the compound **18.** Then, the reaction mixture was acidified by HCl to pH 1 and then refluxed to give compound **19**. $PhPOCl_2$ was chosen as the chloride reagent to synthesize **5b** from **19** because it gave the best yield compared with $POCl_3$ and PCl_5.[16] This route can be scaled to hundred grams that benefits further pharmaceutical research.

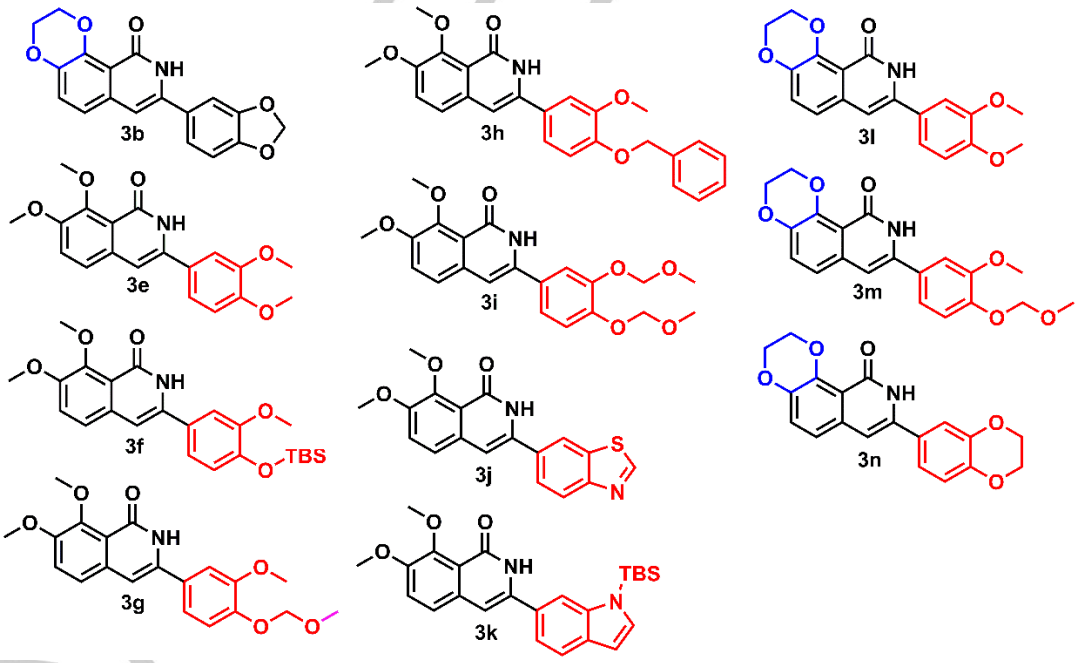

Figure 2. The structures of **3b**, **3e-3n**

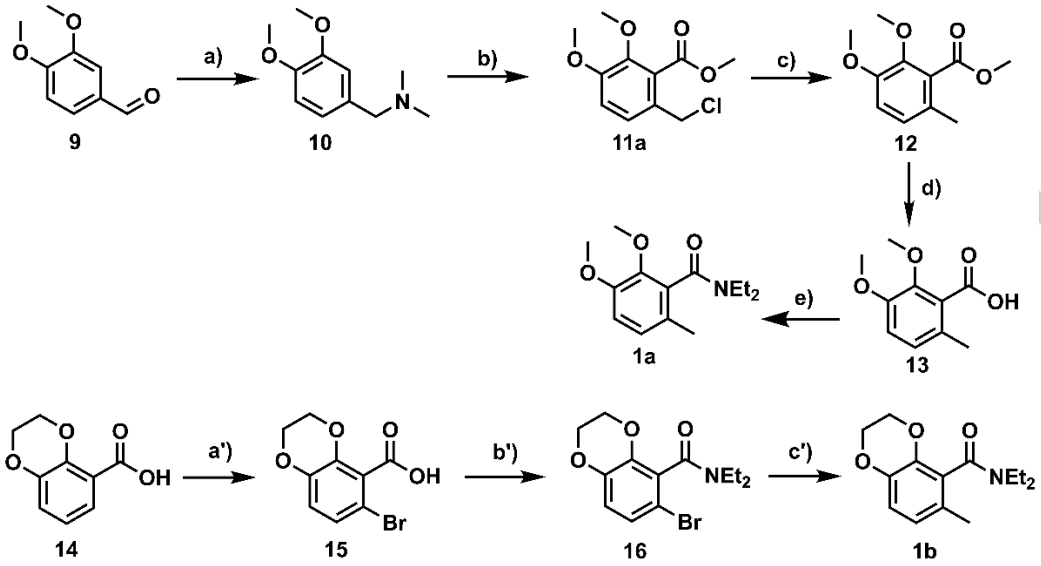

Scheme 2. Synthesis of **1a** and **1b**. Reagents and conditions: a) DMF, HCOOH, 150 °C, 5h; b) n-BuLi (0 °C), CH_3OCOCl (-78 °C), dry THF, r.t. 12h; c) $NaBH_4$ (0 °C), DMSO, r.t. 12h; d) NaOH (10%), MeOH, 100 °C, 12h; e) oxalyl chloride (0 °C), DMF, DCM, diethylamine, r.t. 12h. a') NaOH (0.7M) (0 °C), 1,3-dibromo-5,5-dimethylhydantoin, r.t. 12h; b') oxalyl chloride (0 °C), DMF, DCM, diethylamine, r.t. 12h; c') n-BuLi (-78 °C), dry THF, CH_3I, r.t. 12h.

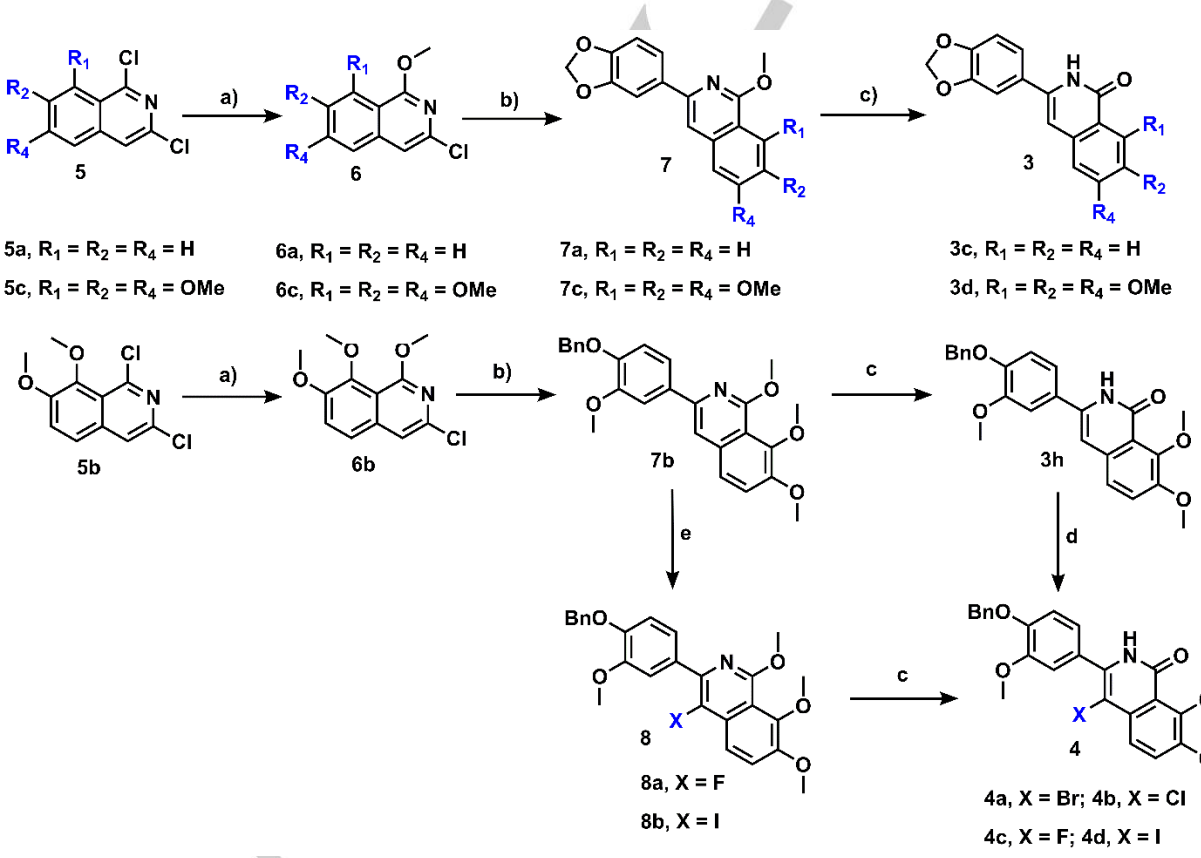

Scheme 3. Synthesis of **4a-4d** and **3c-3d**. Reagents and conditions: a) MeONa, dry 1,4- dioxane, 65 °C, 4h; b) Substituted phenylboronic acid, $Pd_2(dba)_3$, xPhos, K_3PO_4, 1,4- dioxane, 100 °C, 3h; c) HCl (3M), MeOH (100 °C) / TMSCl, NaI, r.t. 3h; d) NBS, THF, r.t. 2h/ NCS, DCM, r.t. 12h; e) Selectfluor, acetonitrile, 70 °C, 2h. / NIS, p-TsOH (0 °C), THF, r.t. 12h.

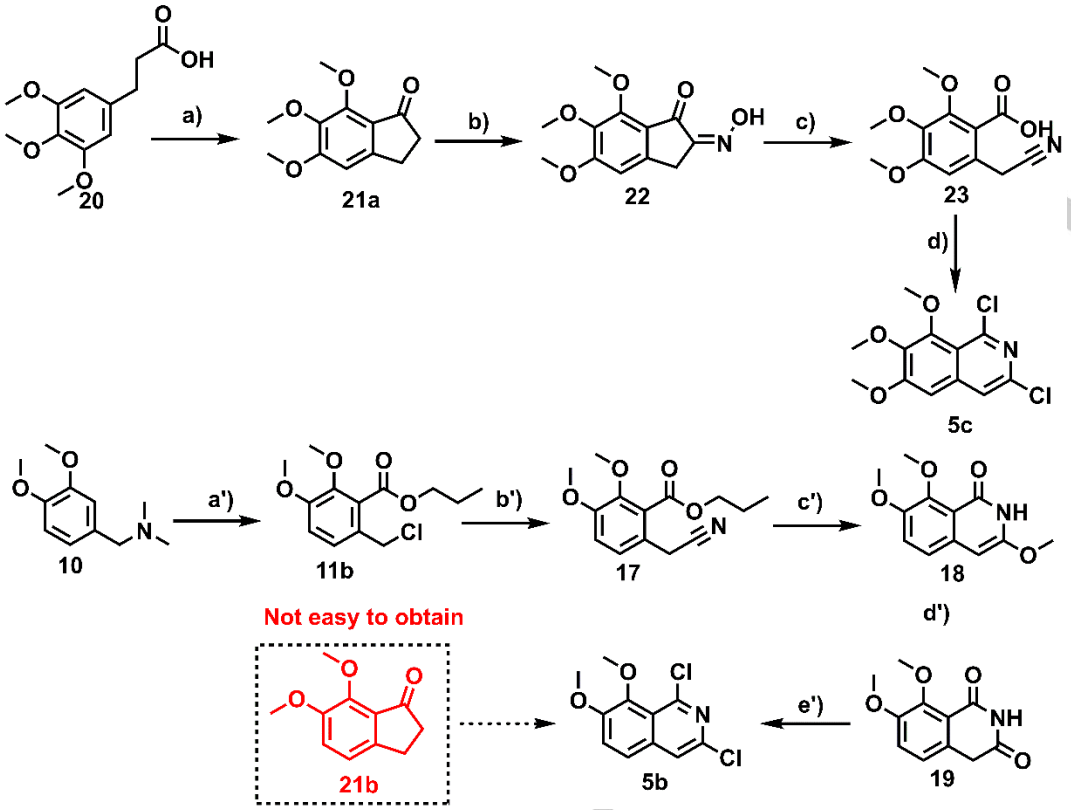

Scheme 4. Synthesis of **5b** and **5c**. Reagents and conditions: a) methanesulfonic acid, P_2O_5, 50 °C, 1h; b) Tert-butyl nitrite, HCl (cat.), MeOH, r.t. 2h. c) NaOH (8%), 50 °C; TsCl, 80 °C, 3h; d) PCl_5, $POCl_3$, 100 °C, 12h. a') n-BuLi (0 °C), C_3H_7OCOCl (-78 °C), dry THF, r.t. 12h; b') TMSCN, TBAF, MeCN, 80 °C, 12h; c') MeONa, dry MeOH, 80 °C 1h; d') MeOH, HCl (3M), 100 °C, 1h; e') $PhP(O)Cl_2$, 160 °C, 3h.

Enzyme inhibition assays

Inhibition assays of hCES (including both hCES1A and hCES2A) by 3-arylisoquinolone analogues were conducted by using fluorescence-based biochemical assays.[17] D-luciferin methyl ester (DME) was used as a probe substrate for hCES1A, while fluorescein diacetate (FD) was used as a specific probe substrate for hCES2A (Table S1).[18] BNPP was used as a positive inhibitor of hCES. LPA was used as a specific inhibitor of hCES2A, while Oleanolic acid (OA) was used as a specific inhibitor of hCES1A (Fig. S1). The IC_{50} values of all tested 3-arylisoquinolone analogues and positive inhibitors were listed in Table 1.

Table 1. The IC_{50} values of 19 3-arylisoquinolones on hCES1A and hCES2A.

Compd.	IC_{50} (μM) for hCES1A	IC_{50} (μM) for hCES2A	Selectivity IC_{50}(hCES2A)/IC_{50}(hCES1A)
3a	>100	12.73 ± 1.67	>7.86
3a'	2.28 ± 0.70	5.90 ± 1.42	0.39
3b	>100	>100	/
3c	>100	>100	/
3d	>100	>100	/
3e	>100	>100	/
3f	>100	>100	/
3g	>100	18.66 ± 6.14	>5.36
3h	>100	0.68 ± 0.07	>147.05
3i	>100	3.84 ± 0.65	>26.04
3j	>100	46.03 ± 31.26	2.17
3k	>100	24.14 ± 9.30	>4.14
3l	>100	23.03 ± 7.79	>4.34
3m	>100	>100	/
3n	>100	>100	/
4a	>100	0.68 ± 0.19	>147.05
4b	>100	4.64 ± 0.80	>21.55
4c	>100	4.084 ± 0.54	>24.47
4d	>100	11.07 ± 0.92	>9.03
BNPP [a]	0.88 ±0.07	6.23 ± 0.90	/
OA [b]	0.084 ± 13.45	/	/
LPA [c]	/	6.85 ± 0.83	/

[a] Bis-p-nitrophenyl phosphate (BNPP), a positive inhibitor of hCEs. [b] Oleanolic acid (OA), a specific inhibitor of hCE1A. [c] loperamide (LPA), as a positive inhibitor of hCE2A.

Initially, compound **3a** exhibited good selectivity and moderate inhibition to hCES2A (hCES1A IC_{50}> 100 μM; hCES2A IC_{50} = 12.73 ± 1.67 μM). While the hydrogen at 2-position was substituted with propyl, the specificity of hCES2A inhibition was lost. The IC_{50} values of **3b**, **3c**, and **3d** showed that the dimethoxy group on the C ring was optimal. A series of compounds (**3e**-**3k**) with various substituents on the A ring showed different inhibitory activity. **3e** and **3f**, substituted by methoxy group and tert-butyldimethylsilyloxy group at 4'-position, respectively, exhibited no inhibition on hCES2A. **3g** and **3h**, substituted by methoxymethoxy group and benzyloxy group at 4'-position, respectively, showed stronger inhibitory effects, especially for **3h** (**3g**: IC_{50} = 18.66 ± 6.14 μM, **3h**: IC_{50} = 0.68 ± 0.07 μM). Therefore, we suggested that the suitable size of the groups at C4'-position on A ring were favored to the inhibitory activity on hCES2A. Compared with **3g**, the IC_{50} value of **3i** increased about 5-fold when the methoxy group at the 3'-position was replaced with the methoxymethoxy group (**3i**: IC_{50} = 3.84 ± 0.65 μM), which also demonstrated that the substituents on A ring were supposed to possess a moderate size. **3k** and **3j** both exhibited moderate inhibition when the 3-position was substituted by benzoheterocyclic groups (**3k**: IC_{50} = 24.14 ± 9.30 μM, **3j**: IC_{50}= 46.03 ± 31.26 μM), suggesting that the introduction of aromatic heterocycles couldn't enhance the inhibition.

In order to further enhance the activity and permeability, we introduced halogen atoms to **3h**. According to the results of bioassay, **4a** showed the equal inhibitory effect to **3h** (**4a**: IC_{50} = 0.68 ± 0.19 μM) (Fig. 3A and 3C). In addition, cell-based inhibition assays demonstrated that both **3h** and **4a** dose-dependently inhibited intracellular hCES2A and **4a** presented better activity on the HepG2 cells (**3h**: IC_{50} = 1.41 ± 0.25 μM; **4a**: IC_{50} = 0.41 ± 0.09 μM) (Fig. 4A and 4B). These results demonstrated that the introduction of the bromine atom may improve the permeability, thereby increasing its activity on cell lines. The inhibition kinetics of **3h** and **4a** against hCES2A-mediated FD hydrolysis were also tested with the K_i values of 0.50 μM and 0.36 μM (Fig. 3B and 3D), respectively.

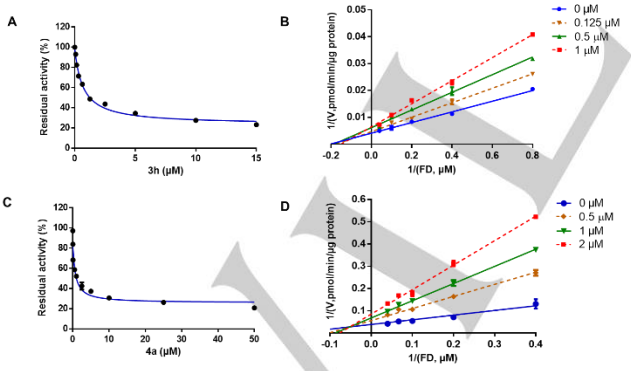

Figure 3. A) The dose-inhibition curve of **3h**; B) The inhibition kinetic plots of **3h** against hCES2A-mediated FD hydrolysis; C) The dose-inhibition curve of **4a**; D) The inhibition kinetic plots of **4a** against hCES2A-mediated FD hydrolysis.

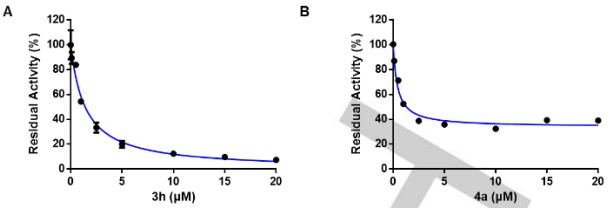

Figure 4. The dose-inhibition curve of **3h** (A) and **4a** (B) against hCES2A-mediated FD hydrolysis in living HepG2 cells.

A summary of the SAR: 1) Dimethoxy groups on the C ring are key groups for hCES2A inhibitory activity. 2) The hydrogen at the 2-position is crucial to the selectivity on hCES2A. 3) The benzyloxy group at the C4' position on the A ring is significant to hCES2A inhibitory activity. 4) The introduction of bromine atom at 4-position of **3h** may enhance the permeability to increase the inhibitory activity on cell lines. (Fig. 5)

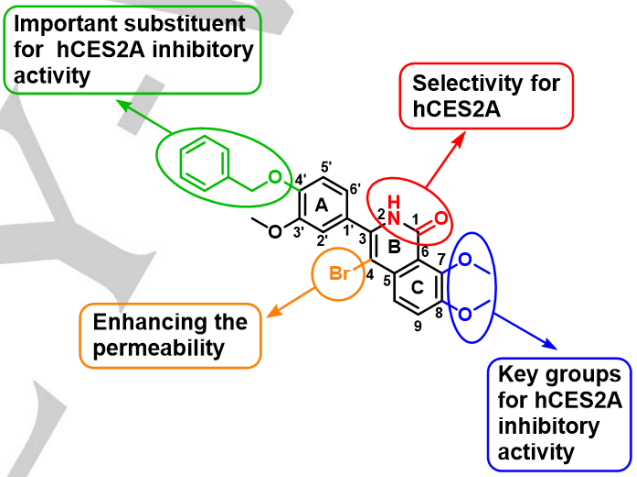

Figure 5. SAR summary of **4a**

Molecular docking simulations

To explore the binding sites of compound **3h** and **4a** with hCES2A, we performed CavityPlus calculation.[19] Based on the ligandability and druggability scores (Table S2), three cavities were predicted as shown in the Fig. 6. We docked compound **3h** and **4a** into the three cavities using Sybyl-Docking Suite embedded in the SYBYL package (Fig. 7, Fig. S3 and S4), the total scores of **3h** and **4a** docking into the three cavities were 9.1024 and 9.0898 (Cavity 1, Active site), 7.1309 and 7.3773 (Cavity 2, Back site), and 6.2895 and 6.4629(Cavity 3, Z site), respectively. The results indicated that compound **3h** and **4a** could bind to multiple sites besides the active sites, resulting in a mixed inhibition manner.

To investigate the specificity of compound **3h**, it was docked into the active pocket of hCES1A and hCES2A using Sybyl-Docking Suite. Compared to hCES1A, **3h** could bind to hCES2A with a relatively higher total score (Table S3), indicating this compound displayed a greater energy advantage over blocking the active site of hCES2A. As shown in Fig. 7B and 7C, two hydrogen bonds of compound **3h** (or **4a)** were formed by NH group and carbonyl oxygen atom on B ring with residue Phe-307 and Met-309,

respectively. In contrast, **3h** didn't have obviously strong interaction with hCES1A, indicating the selectivity of B ring toward hCES2A compared to hCES1A (Fig. S5). In addition, the benzyloxy moiety at C4' position of A ring could interact with the benzene ring of residue Phe-307 via π-π stacking, which was beneficial to the strong inhibitory potency of **3h** (or **4a)** against hCES2A.

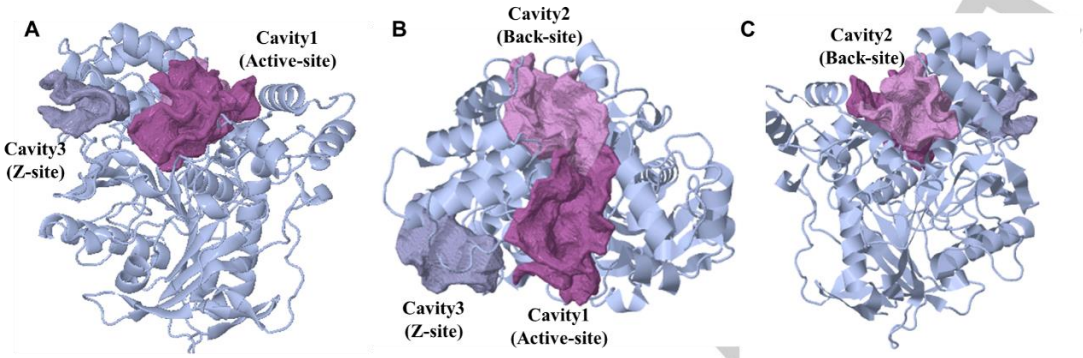

Fig. 6 Three possible binding pockets were predicted with CavityPlus. A) Front view; B) Top view; C) Back view.

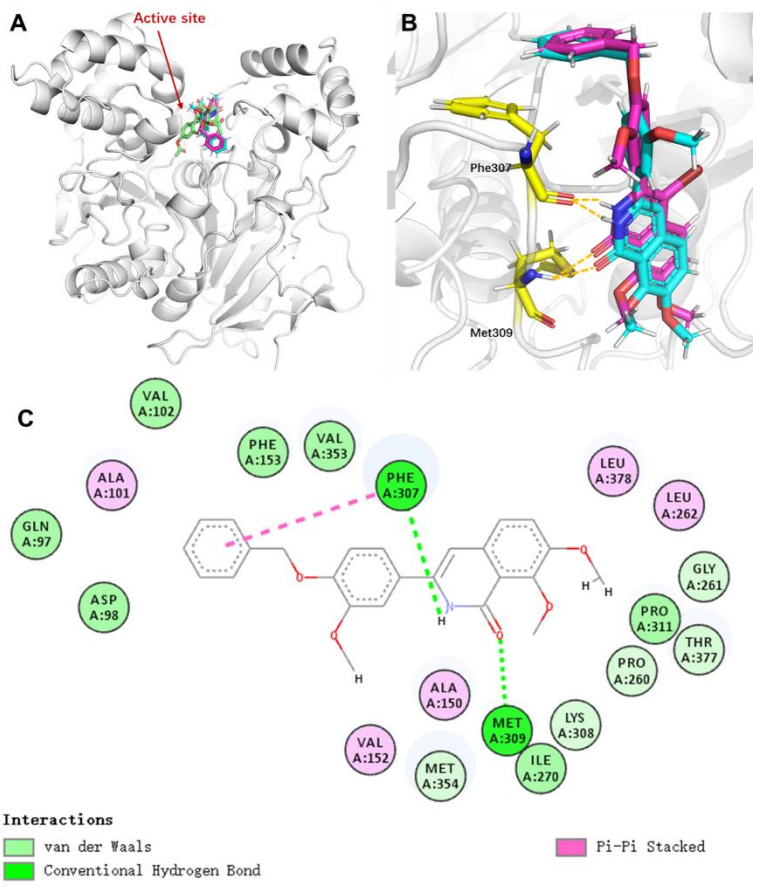

Fig. 7 A) Compound **3h** (blue), **4a** (purple) and substrate FD (green) are partially superimposed in the active site cavity of hCES2A; B) Compound **3h** (blue) and **4a** (purple) could be well docked into the active site cavity of hCES2A; C) The 2D interactions of **3h** with hCES2A.

Conclusion

In summary, a series of 3-arylisoquinolones were synthesized and their inhibitory activities against hCES1A/hCES2A were evaluated. Among all these compounds, **3h** and **4a** exhibited the equal outstanding enzyme inhibitory activity and specificity toward hCES2A with the IC_{50} value of 0.68 μM. Furthermore, **4a** exhibited

3-fold improvement of the inhibition activity in HepG2 cells compared with **3h**. In addition, inhibition kinetics assays and docking calculation demonstrated that compound **3h** and **4a** could bind to multiple sites besides the active sites, functioning as mixed inhibitors. The inhibitory activity and specificity of compound **3h** towards hCES1A and hCES2A was analyzed in detail. All these findings could provide ideal leading compounds for the development of novel hCES2A inhibitors with high potency and excellent specificity in the future.

Experimental

Materials and methods

All starting materials were obtained from commercial suppliers and used without further purification. The ^{1}H NMR and ^{13}C NMR spectra were taken on Bruker Avance-600 or 500 or 400, Varian-MERCURY Plus-600 or 400 NMR spectrometer operating at 600 MHz or 400 MHz for ^{1}H NMR, 125 MHz or 100 MHz for ^{13}C NMR, using TMS as internal standard and $CDCl_3$ or DMSO-d_6 as solvent. ^{13}C NMR spectra were recorded with complete proton decoupling. The ESI-MS or EI-MS was recorded on Finnigan LCQ/DECA or Thermo-DFS, respectively. The HRMS were obtained from Micromass Ultra Q-TOF (ESI) or Thermo- DFS (EI) spectrometer. Flash column chromatography was carried out using silica gel (200~400 mesh). Thin layer chromatography (TLC) was used silica gel F254 fluorescent treated silica which were visualised under UV light (254 nm).
Fluorescein diacetate (FD), Bis-p-nitrophenyl phosphate (BNPP), loperamide (LPA), and Oleanolic acid (OA) and were purchased from TCI (Tokyo, Japan). D-luciferin methyl ester (DME) and N-(2-Butyl-1,3-dioxo-2,3-dihydro-1H-phenalen-6-yl)-2-chloroacetamide (NCEN) were synthesized according to the previously reported schemes.[17a, 20] Luciferin Detection Reagent (LDR) was purchased from Promega Corporation (USA). Pooled human liver microsomes 20 mg/mL (HLMs, from 50 donors, lot no. X008067) were obtained from Bioreclamation IVT (Baltimore, MD, USA) and stored at -80 °C until use. HPLC grade DMSO and acetonitrile were purchased from Tedia (Fairfield, Ohio USA). Phosphate buffer was prepared using Millipore water and then stored at 4 °C until use. Cell culture medium and fetal bovine serum were acquired from Hylcone (Logan, UK). HepG2 cells were purchased from the American Type Culture Collection (Teddington, Middlesex, UK).

Chemistry

General procedure for the preparation of 3b and 3f-3n

To a solution of **1a** (1.0 eq.) in anhydrous tetrahydrofuran (10.0 mL) was added n-BuLi (1.25 eq.) (2.5 M in hexane) at -40 °C under nitrogen for 1h. Then benzonitrile **2** (1.2 eq.) in tetrahydrofuran was added to the reaction mixture dropwise and then the mixture was moved to room temperature and stirred overnight. The reaction mixture was quenched with excess water at room temperature and extracted three times with dichloromethane. The organic layer was washed with water and brine, dried (Na_2SO_4) and evaporated. The residue was separated on silica gel to give the pure product. **3a**, **3a'** and **3e** have reported in our previous work.[9-10]

8-(benzo[d][1,3]dioxol-5-yl)-2,3-dihydro-[1,4]dioxino[2,3-h]isoquinolin-10(9H)-one (3b).

^{1}H NMR (400 MHz, $CDCl_3$) δ 8.86 (s, 1H), 7.22 (d, J = 8.6 Hz, 1H), 7.17 – 7.10 (m, 2H), 7.06 (d, J = 8.6 Hz, 1H), 6.95 – 6.90 (m, 1H), 6.54 (s, 1H), 6.06 (s, 2H), 4.57 – 4.49 (m, 2H), 4.42 – 4.34 (m, 2H). ^{13}C NMR (12 MHz, $CDCl_3$) δ 161.95, 148.68, 148.58, 143.92, 141.36, 137.20, 134.62, 128.29, 123.51, 119.56, 119.14, 114.84, 108.89, 106.20, 103.52, 101.63, 64.86, 63.87. HRMS (ESI): calcd for $C_{18}H_{14}NO_5$ $[M+H]^+$ 324.0866, found: 324.0863.

3-(4-((tert-butyldimethylsilyl)oxy)-3-methoxyphenyl)-7,8-dimethoxyisoquinolin-1(2H)-one (3f).

^{1}H NMR (400 MHz, $CDCl_3$) δ 8.77 (s, 1H), 7.34 (q, J = 8.7 Hz, 2H), 7.12 (dd, J = 2.1, 8.2 Hz, 1H), 7.09 (d, J = 1.9 Hz, 1H), 6.96 (d, J = 8.2 Hz, 1H), 6.58 (s, 1H), 4.00 (s, 3H), 3.98 (s, 3H), 3.92 (s, 3H), 1.04 (s, 9H), 0.21 (s, 6H). ^{13}C NMR (150 MHz, $CDCl_3$) δ 161.65, 151.52, 151.29, 149.75, 146.37, 137.35, 134.05, 127.86, 122.51, 121.48, 119.44, 118.31, 109.29, 102.92, 61.81, 56.90, 55.67, 25.68, 18.49, -4.58. HRMS (ESI): calcd for $C_{24}H_{32}NO_5Si$ $[M+H]^+$ 442.2044, found: 442.2046.

7,8-dimethoxy-3-(3-methoxy-4-(methoxymethoxy)phenyl) isoquinolin-1(2H)-one (3g).

^{1}H NMR (400 MHz, DMSO-d_6) δ 11.05 (s, 1H), 7.52 (d, J = 8.8 Hz, 1H), 7.43 (d, J = 8.8 Hz, 1H), 7.39 (d, J = 2.2 Hz, 1H), 7.30 (dd, J = 2.1, 8.4 Hz, 1H), 7.14 (d, J = 8.5 Hz, 1H), 6.79 (s, 1H), 5.21 (s, 2H), 3.90 (s, 3H), 3.87 (s, 3H), 3.78 (s, 3H), 3.41 (s, 3H). ^{13}C NMR (125 MHz, DMSO-d_6) δ 161.45, 151.19, 150.13, 148.91, 146.87, 137.90, 133.89, 128.35, 123.15, 119.65, 119.61, 119.04, 116.96, 110.89, 102.51, 95.14, 61.43, 56.81, 56.23, 56.14. HRMS (ESI): calcd for $C_{20}H_{22}NO_6$ $[M+H]^+$ 372.1442, found: 372.1445.

3-(4-(benzyloxy)-3-methoxyphenyl)-7,8-dimethoxy-isoquinolin-1(2H)-one (3h).

^{1}H NMR (600 MHz, $CDCl_3$) δ 8.80 (s, 1H), 7.46 (d, J = 7.4 Hz, 2H), 7.39 (t, J = 7.6 Hz, 2H), 7.34 – 7.29 (m, 3H), 7.14 – 7.10 (m, 2H), 6.97 (d, J = 8.8 Hz, 1H), 6.55 (s, 1H), 5.21 (s, 2H), 3.98 (s, 3H), 3.97 (s, 3H), 3.95 (s, 3H). ^{13}C NMR (150 MHz, $CDCl_3$) δ 161.65, 151.34, 150.10, 149.74, 149.15, 137.14, 136.60, 133.97, 128.65, 128.03, 127.40, 127.24, 122.54, 119.42, 118.12, 114.02, 109.05, 103.00, 70.97, 61.81, 56.88, 56.22. HRMS (ESI): calcd for $C_{25}H_{24}NO_5$ $[M+H]^+$ 418.1649, found: 418.1652.

3-(3,4-bis(methoxymethoxy)phenyl)-7,8-dimethoxy-isoquinolin-1(2H)-one (3i).

^{1}H NMR (400 MHz, $CDCl_3$) δ 9.00 (s, 1H), 7.45 (d, J = 1.9 Hz, 1H), 7.38 – 7.31 (m, 2H), 7.28 (dd, J = 1.9, 8.4 Hz, 1H), 7.26 (dd, J = 1.9, 8.4 Hz, 1H), 6.59 (s, 1H), 5.35 (s, 2H), 5.31 (s, 2H), 4.00 (s, 3H), 3.98 (s, 3H), 3.57 (s, 3H), 3.56 (s, 3H). ^{13}C NMR (125 MHz, $CDCl_3$) δ 161.81, 151.43, 149.7 7, 148.19, 147.75, 136.85, 133.97, 128.53, 122.65, 119.78, 119.51, 116.87, 113.94, 103.35, 95.51, 95.29, 61.83, 56.91, 56.39, 56.35. HRMS (ESI): calcd for $C_{21}H_{24}NO_7$ $[M+H]^+$ 402.1547, found: 402.1552.

3-(benzo[d]thiazol-6-yl)-7,8-dimethoxyisoquinolin-1(2H)-one (3j).

^{1}H NMR (400 MHz, $CDCl_3$) δ 9.87 (s, 1H), 9.10 (s, 1H), 8.36 (s, 1H), 8.26 (d, J = 8.4 Hz, 1H), 7.89 (d, J = 8.9 Hz, 1H), 7.38 (s, 2H), 6.76 (s, 1H), 3.99 (s, 3H), 3.96 (s, 3H). ^{13}C NMR (150 MHz, DMSO-d_6) δ 161.33, 157.80, 153.56, 151.53, 148.88, 137.55, 134.56, 133.55, 131.53, 125.28, 123.41, 120.85, 119.59, 104.09, 61.42, 56.77. HRMS (ESI): calcd for $C_{18}H_{15}N_2O_3S$ [M+H]$^+$ 339.0798, found: 339.0801.

3-(1-(tert-butyldimethylsilyl)-1H-indol-6-yl)-7,8-dimethoxy-isoquinolin-1(2H)-one (3k).

^{1}H NMR (400 MHz, $CDCl_3$) δ 8.63 (s, 1H), 7.72 (d, J = 8.3 Hz, 1H), 7.70 (s, 1H), 7.38 – 7.31 (m, 3H), 7.28 (d, J = 3.2 Hz, 1H), 6.66 (dd, J = 0.7, 3.2 Hz, 1H), 6.56 (s, 1H), 4.00 (s, 3H), 3.96 (s, 3H), 0.96 (s, 9H), 0.66 (s, 6H). ^{13}C NMR (150 MHz, $CDCl_3$) δ 161.60, 151.19, 149.76, 141.20, 138.98, 134.27, 132.97, 132.35, 127.76, 122.53, 121.47, 119.41, 117.69, 111.16, 104.95, 103.14, 61.83, 56.94, 26.28, 19.50, 3.80. HRMS (ESI): calcd for $C_{25}H_{31}N_2O_3Si$ 435.2098 [M+H]$^+$, found: 435.2101.

8-(3,4-dimethoxyphenyl)-2,3-dihydro-[1,4]dioxino[2,3-h] isoquinolin-10(9H)-one (3l).

^{1}H NMR (400 MHz, $CDCl_3$) δ 8.69 (s, 1H), 7.24 (d, J = 8.6 Hz, 1H), 7.20 (dd, J = 1.9, 8.1 Hz, 1H), 7.11 (d, J = 2.2 Hz, 1H), 7.08 (d, J = 8.5 Hz, 1H), 6.98 (d, J = 8.1 Hz, 1H), 6.58 (s, 1H), 4.56 – 4.50 (m, 2H), 4.41 – 4.35 (m, 2H), 4.00 (s, 3H), 3.97 (s, 3H). ^{13}C NMR (125 MHz, $CDCl_3$) δ 161.95, 150.15, 149.58, 143.91, 141.33, 137.32, 134.71, 126.85, 123.56, 119.12, 118.23, 114.76, 111.56, 108.56, 103.33, 64.89, 63.87, 56.16, 56.06. HRMS (ESI): calcd for $C_{19}H_{18}NO_5$ 340.1182 [M+H]$^+$, found: 340.1179.

8-(3-methoxy-4-(methoxymethoxy)phenyl)-2,3-dihydro-[1,4]dioxino[2,3-h] isoquinolin-10 (9H)-one (3m).

^{1}H NMR (400 MHz, $CDCl_3$) δ 9.47 (s, 1H), 7.26 (d, J = 8.6 Hz, 1H), 7.25 – 7.18 (m, 3H), 7.08 (d, J = 8.6 Hz, 1H), 6.59 (s, 1H), 5.31 (s, 2H), 4.54 – 4.47 (m, 2H), 4.40 – 4.33 (m, 2H), 4.02 (s, 3H), 3.56 (s, 3H). ^{13}C NMR (150 MHz, $CDCl_3$) δ 162.34, 150.09, 147.49, 143.86, 141.30, 137.52, 134.73, 128.37, 123.53, 119.12, 118.54, 116.36, 114.79, 109.28, 103.58, 95.32, 64.80, 63.86, 56.33, 56.16. HRMS (ESI): calcd for $C_{20}H_{20}NO_6$ 370.1285 [M+H]$^+$, found: 370.1282.

8-(2,3-dihydrobenzo[b][1,4]dioxin-6-yl)-2,3-dihydro-[1,4]dioxino[2,3-h]isoquinolin-10(9H)-one (3n).

^{1}H NMR (400 MHz, $CDCl_3$) δ 8.63 (s, 1H), 7.22 (d, J = 8.6 Hz, 1H), 7.14 (d, J = 2.1 Hz, 1H), 7.11 (dd, J = 2.2, 8.4 Hz, 1H), 7.06 (d, J = 8.7 Hz, 1H), 6.98 (d, J = 8.3 Hz, 1H), 6.55 (s, 1H), 4.54 – 4.49 (m, 2H), 4.40 – 4.35 (m, 2H), 4.33 (s, 4H). ^{13}C NMR (150 MHz, $CDCl_3$) δ 161.84, 144.72, 144.11, 143.91, 141.30, 136.91, 134.68, 127.44, 123.46, 119.15, 118.60, 118.10, 114.83, 114.53, 103.28, 64.86, 64.50, 64.36, 63.86. HRMS (ESI): calcd for $C_{19}H_{16}NO_5$ [M+H]$^+$ 338.1023, found: 338.1027.

4.2.2 General procedure for the preparation of 3c and 3d

A mixture of **7a** or **7b** in methanol (5 mL) and aqueous HCl (3M, 10 mL) was heated at 100 °C for 3 hours. The resulting precipitate was filtered off, washed subsequently with methanol and dichloromethane and dried in vacuo to obtain pure product.

3-(benzo[d][1,3]dioxol-5-yl)isoquinolin-1(2H)-one (3c).

^{1}H NMR (400 MHz, DMSO-d_6) δ 11.43 (s, 1H), 8.18 (d, 1H), 7.75 – 7.64 (m, 2H), 7.47 (ddd, J = 8.2, 6.5, 1.8 Hz, 1H), 7.38 (d, J = 1.9 Hz, 1H), 7.32 (dd, J = 8.2, 1.9 Hz, 1H), 7.04 (d, J = 8.2 Hz, 1H), 6.87 (s, 1H), 6.10 (s, 2H). ^{13}C NMR (125 MHz, DMSO-d_6) δ 163.19, 148.65, 148.17, 140.14, 138.46, 133.06, 128.32, 127.06, 125.03, 121.31, 108.95, 107.44, 103.02, 101.98. HRMS (ESI): calcd for $C_{16}H_{11}NNaO_3$ 288.0631 [M+Na]$^+$, found 288.0634.

3-(benzo[d][1,3]dioxol-5-yl)-6,7,8-trimethoxyisoquinolin-1(2H)-one (3d).

^{1}H NMR (400 MHz, DMSO-d_6) δ 10.97 (s, 1H), 7.34 (d, J = 1.9 Hz, 1H), 7.28 (d, J = 8.1 Hz, 1H), 7.02 (d, J = 7.7 Hz, 2H), 6.72 (s, 1H), 6.10 (d, J = 1.1 Hz, 2H), 3.90 (d, J = 1.0 Hz, 3H), 3.81 (d, J = 1.1 Hz, 3H), 3.77 (d, J = 1.1 Hz, 3H). ^{13}C NMR (125 MHz, DMSO-d_6) δ 160.34, 156.87, 153.69, 148.14, 147.65, 140.99, 139.16, 136.98, 127.54, 120.57, 108.51, 106.76, 103.85, 102.11, 101.54, 61.74, 60.94, 55.86. HRMS (ESI): calcd for $C_{19}H_{18}NO_6$ 356.1129 [M+H]$^+$, found 356.1127.

4.2.3 General procedure for the preparation of 4a and 4b

3-(4-(benzyloxy)-3-methoxyphenyl)-4-chloro-7,8-dimethoxy-isoquinolin-1(2H)-one (4a).

To a solution of **3h** (21 mg, 0.05 mmol) in anhydrous tetrahydrofuran (4 mL) at room temperature was added N-bromosuccinimide (8.9 mg, 0.05 mmol). The mixture was stirred at room temperature for 2h and then poured into water and extracted three times with ethyl acetate. The organic layer was washed with brine, dried (Na_2SO_4) and evaporated. The residue was purified by flash column chromatography to give **4a** as a white solid (15 mg, 61%). ^{1}H NMR (600 MHz, DMSO-d_6) δ 11.27 (s, 1H), 7.73 (d, J = 9.0 Hz, 1H), 7.65 (d, J = 9.1 Hz, 1H), 7.49 (d, 2H), 7.43 (t, J = 8.4, 6.8 Hz, 2H), 7.37 (t, 1H), 7.14 (d, J = 8.4 Hz, 1H), 7.12 (d, J = 2.1 Hz, 1H), 7.06 (dd, J = 8.3, 2.1 Hz, 1H), 5.16 (s, 2H), 3.91 (s, 3H), 3.82 (s, 3H), 3.78 (s, 3H). ^{13}C NMR (125 MHz, DMSO-d_6) δ 159.76, 151.96, 149.09, 148.86, 148.75, 138.56, 137.42, 131.39, 128.92, 128.40, 128.32, 127.81, 122.91, 122.80, 120.30, 119.41, 114.10, 113.01, 97.44, 70.30, 61.44, 56.73, 56.14. HRMS (ESI): calcd for $C_{25}H_{23}BrNO_5$ 496.0754 [M+H]$^+$, found 496.0764.

3-(4-(benzyloxy)-3-methoxyphenyl)-4-bromo-7,8-dimethoxyisoquinolin-1(2H)-one (4b).

To a solution of **3h** (62.3 mg, 0.15 mmol) in dichloromethane (4 mL) at room temperature was added N-chlorosuccinimide (20 mg, 0.15 mmol). The mixture was stirred at room temperature for 2h and then poured into water and extracted three times with ethyl acetate. The organic layer was washed with brine, dried (Na_2SO_4) and evaporated. The residue was purified by flash column chromatography to give **4b** as a white solid (15 mg, 22.3%). ^{1}H NMR (400 MHz, DMSO-d_6) δ 11.28 (d, J = 14.7 Hz, 1H), 7.71 (d, J = 9.0 Hz, 1H), 7.68 – 7.60 (m, 1H), 7.49 (d, J = 7.2 Hz, 2H), 7.42

(t, *J* = 7.4 Hz, 1H), 7.36 (t, *J* = 7.2 Hz, 1H), 7.18 – 6.94 (m, 3H), 5.16 (d, *J* = 4.0 Hz, 2H), 3.90 (d, *J* = 4.5 Hz, 3H), 3.82 (d, *J* = 6.0 Hz, 3H), 3.78 (d, *J* = 5.1 Hz, 3H). ^{13}C NMR (150 MHz, DMSO-d_6) *δ* 159.62, 152.07, 149.21, 148.88, 148.79, 137.42, 136.46, 130.48, 128.94, 128.42, 128.39, 128.33, 125.82, 122.90, 120.06, 119.40, 113.97, 113.01, 106.32, 70.25, 61.46, 56.71, 56.09. HRMS (ESI): calcd for $C_{25}H_{23}ClNO_5$ 452.1259 [M+H] $^+$, found 452.1291.

General procedure for the preparation of 4c and 4d

To a solution of **8b** or **8b** (1.0 eq.) in anhydrous acetonitrile was added sodium iodide (3 eq.) followed by chlorotrimethylsilane (1.7 eq.) and the mixture was stirred at room temperature for **3h** and then poured into water and extracted three times with ethyl acetate. The organic layer was washed with brine, dried (Na_2SO_4) and evaporated. The residue was purified by flash column chromatography to give the pure product.

3-(4-(benzyloxy)-3-methoxyphenyl)-4-fluoro-7,8-dimethoxy-isoquinolin-1(2H)-one (4c).

^{1}H NMR (600 MHz, DMSO-d_6) *δ* 10.92 (s, 1H), 7.64 (d, *J* = 9.0 Hz, 1H), 7.52 (d, *J* = 8.8 Hz, 1H), 7.48 (d, *J* = 7.0 Hz, 2H), 7.42 (t, *J* = 7.6 Hz, 2H), 7.36 (t, 1H), 7.25 (d, *J* = 2.1 Hz, 1H), 7.20 (d, 1H), 7.16 (d, *J* = 8.5 Hz, 1H), 5.16 (s, 2H), 3.91 (s, 3H), 3.86 (s, 3H), 3.80 (s, 3H). ^{13}C NMR (150 MHz, DMSO-d_6) *δ* 159.27, 152.38, 149.34, 149.16, 148.78, 137.36, 128.93, 128.41, 128.30, 125.84, 125.70, 121.92, 121.89, 119.57, 116.07, 116.03, 113.49, 112.67, 70.26, 61.54, 56.80, 56.03, 49.07. HRMS (EI): calcd for $C_{25}H_{22}FNO_5$ 435.1477 [M]$^+$, found 435.1474.

3-(4-(benzyloxy)-3-methoxyphenyl)-4-iodo-7,8-dimethoxy-isoquinolin-1(2H)-one (4d).

^{1}H NMR (600 MHz, DMSO-d_6) *δ* 11.27 (s, 1H), 7.71 (d, *J* = 9.0 Hz, 1H), 7.63 (d, *J* = 9.2 Hz, 1H), 7.49 (d, 2H), 7.42 (t, 2H), 7.37 (t, 1H), 7.13 (d, *J* = 8.3 Hz, 1H), 7.05 (d, *J* = 2.1 Hz, 1H), 6.97 (dd, *J* = 8.2, 2.1 Hz, 1H), 5.15 (s, 2H), 3.90 (s, 3H), 3.81 (s, 3H), 3.77 (s, 3H). ^{13}C NMR (125 MHz, DMSO-d_6) *δ* 160.07, 151.69, 148.78, 148.67, 142.63, 137.42, 133.40, 131.25, 128.92, 128.41, 128.35, 128.08, 122.92, 119.60, 119.37, 114.18, 112.94, 70.31, 61.43, 56.71, 56.15. HRMS (EI): calcd for $C_{25}H_{22}INO_5$ 543.0537 [M] $^+$, found 543.0547.

Biological assays

Enzyme inhibition assays

FD, In this study, hCES2A inhibition assay was conducted using FD as a specific fluorescent probe substrate for hCES2A.[17b, 21] Briefly, the incubation mixture (200 μL) contained each tested compound, HLM (2 μg/mL), and PBS (pH 7.4). After 3 min pre-incubated at 37 °C, the hydrolytic reaction was started by addition of the substrate (FD), and then the mixture was incubated at 37 °C for 30 min. The fluorescent signal of FD hydrolytic products was analyzed by the microplate reader (SpectraMax® iD3, Molecular Devices, Austria), and more details were shown in Table S1. The dose-inhibition curve of 10 3-arylisoquinolones were shown in Fig. S2.

For hCES1A inhibition assay, DME (an optical substrate for hCES1A) was used as a specific probe substrate for hCES1A.[17a] In short, an incubation mixture (100 μL) contained HLM (1 μg/mL), PBS (pH 6.5), each tested compound was pre-incubated for 3 min at 37 °C. After then, the hydrolytic reaction was started by addition of DME, and then the mixture was incubated at 37 °C for 10 min. After that, equal volume of LDR was added to stop reaction. The detection conditions and more information were depicted in Table S1.

Cell inhibition assay

NCEN, a two-photon fluorescent substrate for highly selective and sensitive sensing of hCES2A, which was used for sensing of intracellular hCES2A in living cells.[20] In brief, HepG2 cells were cultured in DMEM medium supplemented with 10% fetal bovine serum, 100 U/mL penicillin and 100 μg/mL streptomycin. Cells were seeded in triplicate on 96-well plates at a density of 1×104 per well and incubated overnight to ensure cell adhesion. The cells were then treated with a series of concentrations of **3h** or **4a** and incubated for 30 min at 37 °C under 5% CO_2. To measure the hydrolytic activity of intracellular CES2A, HepG2 cells were treated with NCEN (10 μM) for 50 min in the presence of Hoechst 33342 (1 μM), then washed, and analyzed by using a microplate reader (Spectra Max® iD3, Molecular Devices, Austria). The fluorescence detection conditions were depicted in Table S1.

Determination of Inhibition Constant

The inhibition constant (K_i) values of **4a** and **3h** against hCES2A were determined by a panel of inhibition kinetic assays, using varied concentrations of FD and various doses of **4a** or **3h**. Line weaver-Burk plots were plotted by GraphPad Prism 7.0, while the second plot of the slopes from Lineweaver-Burk plots were used to determine the inhibition constant (K_i) values of each inhibitor.[22] All inhibition kinetic data were fitted by the following equations for competitive inhibition Eq. (1), non-competitive inhibition Eq. (2), and mixed inhibition Eq. (3)

$$V=(V_{max}S)/\,[K_m\,(1+I/\,K_i)\,+S] \quad (1)$$

$$V=(V_{max}S)/\,[(K_m\,+S)\,\times\,(1+I/\,K_i)] \quad (2)$$

$$V=(V_{max}S)/\,[(K_m\,+S)\,\times(1+I/\alpha K_i)] \quad (3)$$

where V is the hydrolytic velocity of FD, V_{max} is the maximum velocity. S and I are the concentration of substrate and inhibitor, respectively. K_i is the inhibition constant, K_m is the Michaelis-Menten constant (the substrate concentration at half of the V_{max}).

Statistical Analysis

The residual activities of enzyme were calculated with the following formula: the residual activity (%) = (the florescence intensity in the presence of inhibitor)/the florescence intensity in negative control × 100%. All assays were conducted in triplicate, and the data were shown as mean ± SD. The IC_{50} values and the K_i values were evaluated by nonlinear regression using Graph Pad Prism 7.0 software (GraphPad Software, Inc., La Jolla, USA).

Molecular docking simulations

The structure of hCES2A was downloaded from the SWISS-MODEL library (a database of annotated 3D protein structure models generated by homology modeling pipeline)[23] applying for carrying out calculation. Molecular docking was performed utilizing Sybyl-Docking Suite embedded in SYBYL-X 2.0.[24] The protein was assigned hydrogens, Kollman United/Kollman all-atom force field, and standard AMBER atomic partial charges. The docking 'Protomol' was generated adopting default parameters. The prepared ligand structures were docked by Surflex dock program. The docking simulation was carried out based on the conjugate minimization methodology of Powell. The protein-ligand poses with high total scores were displayed.

Acknowledgments

This work was supported by the National Key Research and Development Program of China [2016YFA0502301, 2017YFC1700200, 2017YFC1702000], National Major Scientific and Technological Special Project for "Significant New Drugs Development" (2018ZX09711002), Natural Science Foundation of China [81922070, 81973286, 81973393],Natural Science Foundation of Shanghai, China (19ZR1467800), and Program of Shanghai Academic/Technology Research Leader [18XD1403600].

Declaration of Interest

The authors state that no conflicts of interest exist.

Keywords: 3-arylisoquinolone • hCES2A • specific • structure-activity relationship

References:

[1] a) D. Wang, L. Zou, Q. Jin, J. Hou, G. Ge, L. Yang, *Acta Pharm. Sin. B* **2018**, *8*, 699-712; b) L. W. Zou, Q. Jin, D. D. Wang, Q. K. Qian, D. C. Hao, G. B. Ge, L. Yang, *Curr. Med. Chem.* **2018**, *25*, 1627-1649; c) S. P. Sanghani, P. C. Sanghani, M. A. Schiel, W. F. Bosron, *Protein Pept. Lett.* **2009**, *16*, 1207-1214; d) D. D. Wang, L. W. Zou, Q. Jin, J. Hou, G. B. Ge, L. Yang, *Fitoterapia* **2017**, *117*, 84-95.

[2] T. Imai, *Drug Metab. Pharmacokinet.* **2006**, *21*, 173-185.

[3] a) N. Ribelles, J. Lopez-Siles, A. Sanchez, E. Gonzalez, M. J. Sanchez, F. Carabantes, P. Sanchez-Rovira, A. Marquez, R. Duenas, I. Sevilla, E. Alba, *Curr. Drug Metab.* **2008**, *9*, 336-343; b) G. Xu, W. Zhang, M. K. Ma, H. L. McLeod, *Clin. Cancer Res.* **2002**, *8*, 2605-2611.

[4] S. C. Laizure, V. Herring, Z. Hu, K. Witbrodt, R. B. Parker, *Pharmacotherapy* **2013**, *33*, 210-222.

[5] a) M. K. Ma, H. L. McLeod, *Curr. Med. Chem.* **2003**, *10*, 41-49; b) S. K. Quinney, S. P. Sanghani, W. I. Davis, T. D. Hurley, Z. Sun, D. J. Murry, W. F. Bosron, *J. Pharmacol. Exp. Ther.* **2005**, *313*, 1011-1016.

[6] J. L. Hyatt, L. Tsurkan, M. Wierdl, C. C. Edwards, M. K. Danks, P. M. Potter, *Mol. Cancer Ther.* **2006**, *5*, 2281-2288.

[7] R. M. Wadkins, J. L. Hyatt, X. Wei, K. J. Yoon, M. Wierdl, C. C. Edwards, C. L. Morton, J. C. Obenauer, K. Damodaran, P. Beroza, M. K. Danks, P. M. Potter, *J. Med. Chem.* **2005**, *48*, 2906-2915.

[8] D. B. Khadka, S. H. Yang, S. H. Cho, C. Zhao, W. J. Cho, *Tetrahedron* **2012**, *68*, 250-261.

[9] B. Li, G. Wang, M. Yang, Z. Xu, B. Zeng, H. Wang, J. Shen, K. Chen, W. Zhu, *Eur. J. Med. Chem.* **2013**, *70*, 677 - 684.

[10] B. Li, G. Wang, Z. Xu, Y. Zhang, X. Huang, B. Zeng, K. Chen, J. Shi, H. Wang, W. Zhu, *Eur. J. Med. Chem.* **2014**, *77*, 204 - 210.

[11] a) P. M. Potter, R. M. Wadkins, *Curr. Med. Chem.* **2006**, *13*, 1045-1054; b) S. Bencharit, C. C. Edwards, C. L. Morton, E. L. Howard-Williams, P. Kuhn, P. M. Potter, M. R. Redinbo, *J. Mol. Biol.* **2006**, *363*, 201-214; c) C. T. Prabhakara, S. A. Patil, S. S. Toragalmath, S. M. Kinnal, P. S. Badami, *J. Photochem. Photobiol., B* **2016**, *157*, 1-14.

[12] a) E. L. Eliel, T. N. Ferdinand, S. M. C. Herrmann, *J. Org. Chem.* **1954**, *19*, 1693-1698; b) T. N. Le, W. J. Cho, *Chem. Pharm. Bull.* **2005**, *53*, 118-120.

[13] P. M. Léo, C. Morin, C. Philouze, *Org. Lett.* **2002**, *4*, 2711-2714.

[14] S. R. Haadsma-Svensson, K. A. Cleek, D. M. Dinh, J. N. Duncan, C. L. Haber, R. M. Huff, M. E. Lajiness, N. F. Nichols, M. W. Smith, K. A. Svensson, M. J. Zaya, A. Carlsson, C.-H. Lin, *J. Med. Chem.* **2001**, *44*, 4716-4732.

[15] G. Simchen, *Angew. Chem., Int. Ed. Engl.* **1966**, *5*, 663-663.

[16] S. Sundriyal, P. B. Chen, A. S. Lubin, G. A. Lueg, F. Li, A. J. P. White, N. A. Malmquist, M. Vedadi, A. Scherf, M. J. Fuchter, *MedChemComm* **2017**, *8*, 1069-1092.

[17] a) D. D. Wang, Q. Jin, L. W. Zou, J. Hou, X. Lv, W. Lei, H. L. Cheng, G. B. Ge, L. Yang, *Chem. Commun. (Cambridge, U. K.)* **2016**, *52*, 3183-3186; b) J. Wang, E. T. Williams, J. Bourgea, Y. N. Wong, C. J. Patten, *Drug Metab. Dispos.* **2011**, *39*, 1329-1333.

[18] Z. M. Weng, G. B. Ge, T. Y. Dou, P. Wang, P. K. Liu, X. H. Tian, N. Qiao, Y. Yu, L. W. Zou, Q. Zhou, W. D. Zhang, J. Hou, *Bioorg. Chem.* **2018**, *77*, 320-329.

[19] Y. Xu, S. Wang, Q. Hu, S. Gao, X. Ma, W. Zhang, Y. Shen, F. Chen, L. Lai, J. Pei, *Nucleic Acids Res.* **2018**, *46*, W374-W379.

[20] Q. Jin, L. Feng, D. D. Wang, Z. R. Dai, P. Wang, L. W. Zou, Z. H. Liu, J. Y. Wang, Y. Yu, G. B. Ge, J. N. Cui, L. Yang, *ACS Appl. Mater. Interfaces* **2015**, *7*, 28474-28481.

[21] L. Ding, L. Wang, K. Zou, B. Li, Y. Song, Q. Zhang, Y. Zhao, Z. Xu, G. Ge, B. Zhao, W. Zhu, *RSC Adv.* **2019**, *9*, 35904-35912.

[22] Y.-Q. Wang, Z.-M. Weng, T.-Y. Dou, J. Hou, D.-D. Wang, L.-L. Ding, L.-W. Zou, Y. Yu, J. Chen, H. Tang, G.-B. Ge, *Int. J. Biol. Macromol.* **2018**, *120*, 1944-1954.

[23] A. Waterhouse, M. Bertoni, S. Bienert, G. Studer, G. Tauriello, R. Gumienny, F. T. Heer, T. A. P. de Beer, C. Rempfer, L. Bordoli, R. Lepore, T. Schwede, *Nucleic Acids Res.* **2018**, *46*, W296-W303.

[24] A. Ragunathan, K. Malathi, S. Ramaiah, A. Anbarasu, *J. Cell. Biochem.* **2019**, *120*, 7751-7758.

Entry for the Table of Contents

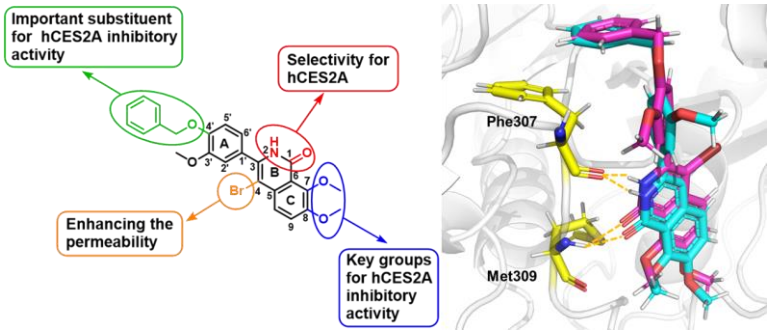

3-arylisoquinolone analogues **3h** and **4a** could potently and specifically inhibit hCES2A (hCES2A: IC_{50} = 0.68μM; hCES1A: IC_{50} > 100μM). Moreover, **4a** exhibited 3-fold improvement inhibition on intracellular hCES2A in living HepG2 cells compared with **3h**, with the IC_{50} value of 0.41 μM. The inhibitory activity and specificity of active compounds was revealed by structure-activity relationship analyzes and docking studies.